EPJ Web of Conferences **69**, 00024 (2014)
DOI: 10.1051/epjconf/20146900024

Comparison of approximations to the transition rate in the DDHMS preequilibrium model

L. Brito[1,a] and B. V. Carlson[1]

[1] *Instituto Tecnológico de Aeronáutica, São José dos Campos SP Brasil*

Abstract. The double differential hybrid Monte Carlo simulation model (DDHMS) originally used exciton model densities and transition densities with approximate angular distributions obtained using linear momentum conservation. Because the model uses only the simplest transition rates, calculations using more complex approximations to these are still viable. We compare calculations using the original approximation to one using a nonrelativistic Fermi gas transition densities with the approximate angular distributions and with exact nonrelativistic and relativistic transition transition densities.

1 Introduction

The hybrid Monte Carlo simulation model[1] was proposed by Blann as a substitute for the exciton and hybrid preequilibrium reaction models, which depend on the overly strong hypothesis of equal a priori occupation of all n exciton states. It takes into account only two-body collisions creating independent particle-hole pairs and the subsequent emission of particles. Nevertheless, it provides a better approximation to the early stages of a preeequilibrium reaction than its predecessors.[2] The model was extended by Blann and Chadwick to calculate double differential spectra (DDHMS) using approximate expressions obtained from considerations of linear momentum conservation for the energy-dependent angular distributions of the particles and holes created.[4, 5]

Because the DDHMS uses only two-body transitions to two-particle-one-hole (2p-1h) or one-hole-two-particle (1h-2p) states, the transitions can be calculated in more complex approximations than that used in the original work. The simplest extension would be to substitute the exciton model densities and transition rates, based on equally spaced levels, with Fermi gas densities and transition rates that better reflect the nuclear single-particle density of states. In this context, however, the transition rates and densities correlated in energy and angle can also be calculated directly,[6] along the lines of work developed long ago by Kikuchi and Kawai.[7]

2 Formalities

Making use Fermi's golden rule, the differential rate of creation of nucleon particle-hole pairs by a nucleon of momentum p_1 passing through nuclear matter is given by

$$\frac{d\Gamma_1^{\downarrow}(\vec{p}_1)}{\hbar} = \frac{2\pi}{\hbar}|\langle\vec{p}_1\vec{p}_2|U|\vec{p}_3\vec{p}_4\rangle|^2\, d\rho_{1p\to 2p1h}(\vec{p}_1, \vec{p}_2\vec{p}_3\vec{p}_4)\,, \tag{1}$$

[a] e-mail: britoluc@ita.br

where the differential density of available states is determined by the initial density of states at momentum $\vec{p}_2$ in the Fermi sea and the final densities of states at momenta $\vec{p}_3$ and $\vec{p}_4$ above the Fermi level, subject to the constraints of energy and momentum conservation,

$$d\rho_{1p\to 2p1h}(\vec{p}_1,\vec{p}_2\vec{p}_3\vec{p}_4) = V^2\,(2\pi\hbar)^3\,\delta\left(\vec{p}_1+\vec{p}_2-\vec{p}_3-\vec{p}_4\right)\delta\left(e(p_1)+e(p_2)-e(p_3)-e(p_4)\right) \times\theta\left(p_{F2}-\left|\vec{p}_2\right|\right)\frac{d^3p_2}{(2\pi\hbar)^3}\theta\left(\left|\vec{p}_3\right|-p_{F1}\right)\frac{d^3p_3}{(2\pi\hbar)^3}\theta\left(\left|\vec{p}_4\right|-p_{F2}\right)\frac{d^3p_4}{(2\pi\hbar)^3}\,, \quad (2)$$

where V is the nuclear volume and p_{F1} and p_{F2} are the Fermi energies corresponding to the two particles in the collision ($p_1 \to p_3$ and $p_2 \to p_4$).

If we assume that the matrix element is isotropic and energy-independent, we can perform the integrals to obtain an exact expression for the width $\Gamma_1^{\downarrow}(\vec{p}_1)$ in terms of the density $\rho_{1p\longrightarrow 2p1h}(\vec{p}_1)$, which in this case is the density of states available from the state of linear momentum $\vec{p}_1$. An analysis of the linear momentum conserving delta functions permits a reduction of the available density of states to

$$\rho_{1p\to 2p1h}(\vec{p}_1) = \frac{4V^2}{(2\pi)^4\hbar^6}\int\frac{1}{|\vec{p}_1+\vec{p}_2|}\delta\left(|\vec{p}_1+\vec{p}_2|^2-|\vec{p}_3+\vec{p}_4|^2\right) \times\delta\left(e(p_1)+e(p_2)-e(p_3)-e(p_4)\right)\theta(p_{F2}-p_2)\theta(p_3-p_{F1})\theta(p_4-p_{F2}) \times p_2^2\,dp_2\,d\cos\theta_{12}\,p_3^2\,dp_3\,p_4^2\,dp_4\,d\cos\theta_{34}\,, \quad (3)$$

where θ_{12} and θ_{34} are the angles between $\vec{p}_1$ and $\vec{p}_2$ and between $\vec{p}_3$ and $\vec{p}_4$, respectively. The remaining integrals can be performed analytically for both nonrelativistic energies ($e(p) = p^2/2m$)[6] and relativistic ones ($e(p) = \sqrt{p^2+m^2}$)[8]. The partial integrals furnish distributions of the variables that permit their efficient Monte Carlo sampling in both the relativistic and nonrelativistic cases.

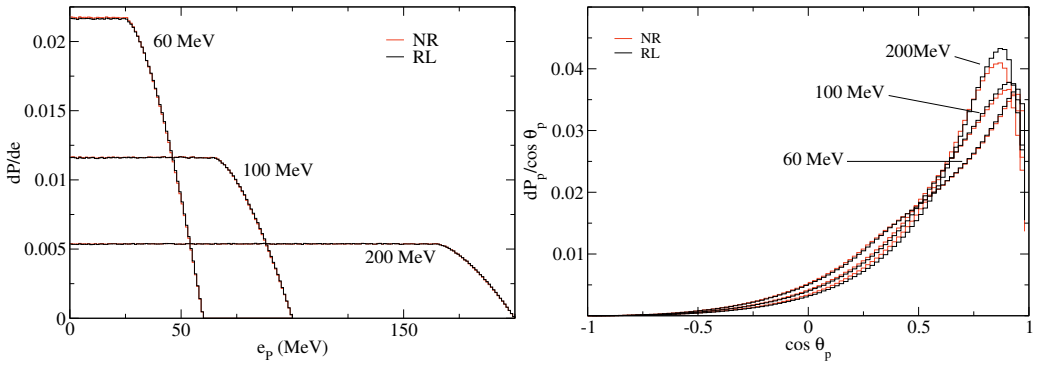

Figure 1. (a) Distribution of final particle energy for initial energies of 60, 100 and 200 MeV. (b) Distribution of final particle scattering angle for initial energies of 60, 100 and 200 MeV.

3 Results and discussion

We begin by comparing the exact relativistic and nonrelativistic Fermi gas distributions. The exciton model distributions were compared to the exact nonrelativistic Fermi gas ones in Ref. [6]. In Fig.

1a, we show the energy distribution of the particles at three values of the incident energy. Both incident and final energies are with respect to the Fermi energy. The relativistic and nonrelativistic energy distributions are almost indistinguishable. They are also extremely similar to the exciton model distributions. Due to the limited number of hole states, the energy distributions all display the same plateau up to the energy $e(p_1) - e_{F2}$, above which they fall more or less linearly to zero.

The angular distribution of the final particles is shown in Fig. 1b. At the lowest energy, 60 MeV, the relativistic and nonrlativistic curves are indistinguishable, as one would expect. As the energy increases, the curves become more forward peaked, with the relativistic distribution slightly more forward peaked than the nonrelativistic one. The can be understood in terms of the Lorentz factor, which effectively increases the mass of the incident particle and reduces the scattering angle.

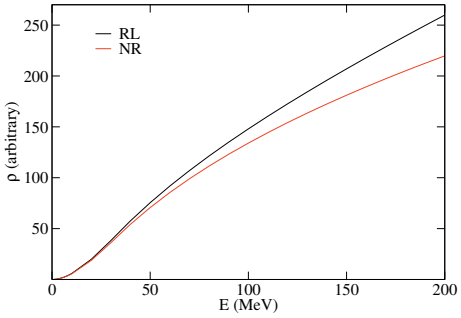

Figure 2. Density of available states for the relativistic and nonrelativistic Fermi gas as a function of the incident energy with respect to the Fermi energy, in arbitrary units.

In Fig. 2, we compare the densities of available states of the relativistic and nonrelativistic Ferm gases. We note that the two coincide at low energy, as would be expected but that the relativistic density increases faster with the energy and is almost 20% larger at 200 MeV. The use of the relativistic density of available states will thus increase the scattering and decrease the emission of more energetic particles when compared to the nonrelativistic one.

We also compare the double-differential cross sections obtained using the the various approximations to the transition densities as implemented in the DDHMS module of the EMPIRE-3.1 reaction code.[9] In Fig 3, we show calculations using 1) exciton model transition densities with approximate angular distributions (ED); 2) Fermi gas transition densities with approximate angular distributions (FGD); 3) exact nonrelativistic Fermi gas transition densities ((EFGD); and 4) exact relativistic Fermi gas transition densities ((ERFGD), as well as experimental data from Ref. [10]. The figure compares the calculations with the experimental data at three angles for each of the three reactions, protons incident on ^{54}Fe at 28 Mev and incident on ^{56}Fe and ^{120}Sn at 62 MeV.

We see that the exciton density, Fermi gas density and exact relativistic Fermi gas density describe the data fairly well at mid and backward angles. The exact nonrelativistic density also shows reasonable agreement with the data at mid angles but decreases too quickly with energy at back angles. It is also higher than the other transition densities at forward angles. As the energies here are strictly nonrelativistic, we would expect the exact nonrelativistic and relativistic calculations to coincide. As they do not, we suspect that there is something amiss with our implementation of the nonrelativistic Fermi gas in the DDHMS module of EMPIRE-3.1. We note that none of the models show reasonable agreement with the high energy part of the spectrum at forward angles. This is due to the fact that

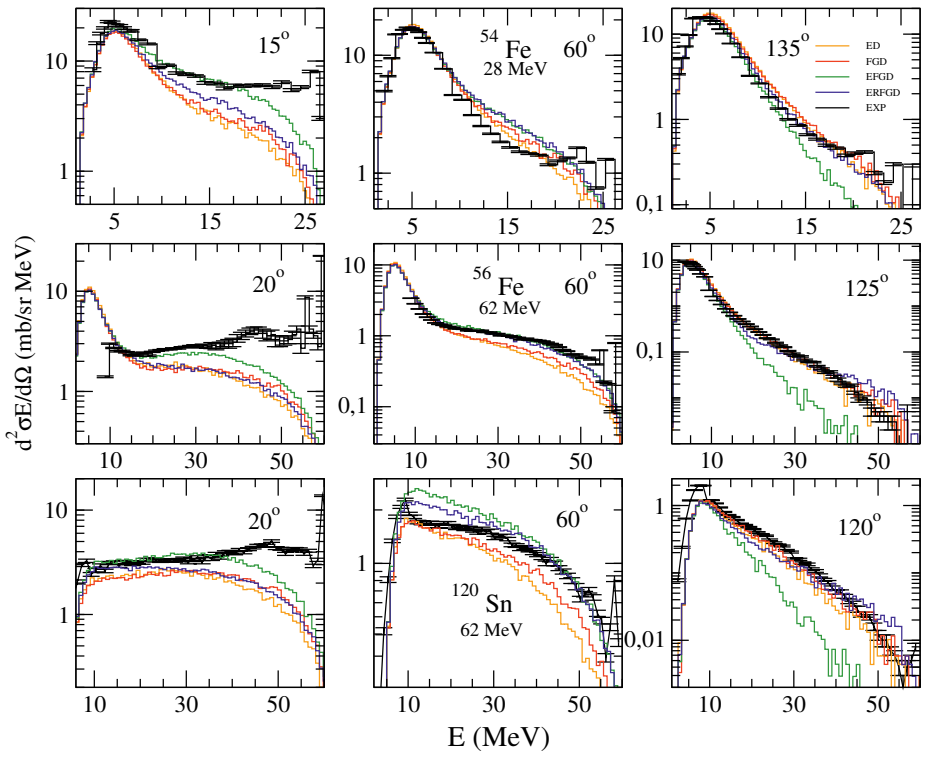

Figure 3. Proton emission spectra from the reactions of 28-MeV protons on ^{54}Fe, at 20°, 60° at 125°, and of 62-MeV protons on ^{56}Fe and ^{120}Sn, at 20°, 60° at 135° and 20°, 60° at 120°, respectively. The histograms are explained in the text. The experimental data were taken from Ref.[10].

the DDHMS is limited to a semiclassical description of particle-hole modes, while the low excitation nuclear spectrum, corresponding to high emission energy, is dominated by quantum collective modes.[11, 12]

In conclusion, we have compared exact relativistic and nonrelativistivc Fermi gas transition densities and found that the relativistic density furnishes more scattering and less emission at higher energies. The scattering is also more forward peaked with the relativistic densities. We have implemented the exact densities in the DDHMS module of the EMPIRE -3.1 code and have compared the double differential spectra provided by the exact and approximate transition densities for three nuclei. We find the agreement generally good for mid and backward angles. None of the calculations can reproduce the high energy component of forward angle scattering, which is dominated by scattering from collective states. Discrepancies between the two exact transition densities led us to conclude that there is an error in our implementation of the exact nonrelativistic Fermi gas density. We plan to correct this in the near future and to continue the comparison between transition densities at higher energies.

LB acknowledges the support of CAPES. BVC acknowledges partial support from FAPESP, CAPES and the CNPq.

References

[1] M. Blann, Rev. C 54 (1996) 1341.
[2] C.A. Soares Pompeia and B. V. Carlson, Phys. Rev. C 74 (2006) 054609.
[3] M. Blann and M. B. Chadwick, Phys. Rev. C 57 (1998) 233.
[4] M. B. Chadwick and P. Oblozinsky, Phys. Rev. C 46 (1992) 2028.
[5] M. B. Chadwick and P. Oblozinsky, Phys. Rev. C 50 (1994) 2490.
[6] D. F. Mega and B. V. Carlson, EPJ Web of Conferences 21 (2012) 09001.
[7] K. Kikuchi and M. Kawai, *Nuclear Matter and Nuclear Reactions*, (North-Holland, Amsterdam, 1968).
[8] L. Brito, D. F. Mega and B. V. Carlson, AIP Conf. Proc. 1529 (2013) 287.
[9] M. Herman *et al.* EMPIRE-3.1, available online at http://www.nndc.bnl.gov/empire/.
[10] F. Bertrand and R. Peelle, Phys. Rev. C 8 (1973) 1045.
[11] T. Tamura, T. Udagawa and H. Lenske, Phys. Rev. C 26 (1982) 379.
[12] M. Dupuis, T. Kawano, J.-P. Delaroche, E. Bauge, Phys. Rev. 83 (2011) 014602.